ACOUSTICS 2012

Effect of contact with an elastic wall on the spectral characteristics of the scattered echo of a contrast microbubble

A. A. Doinikov, L. Aired and A. Bouakaz

INSERM U930 CNRS ERL3106, Université François Rabelais, CHU Bretonneau, 2 Blvd. Tonnellé, 37044 Tours, France
doinikov@bsu.by

A Rayleigh-Plesset-like equation is derived to model the radial oscillation of a contrast agent microbubble attached to an elastic wall. The derived equation shows that contact with the wall affects the bubble oscillation as if the bubble oscillated in a liquid with a changed (effective) density. As a result, depending on the wall properties, the resonance frequency and the oscillation amplitude of the attached bubble can be either lower or higher than those of the same bubble in an unbounded liquid. Numerical simulations were made to investigate the acoustic response of an attached contrast microbubble. It was assumed that the bubble shell properties are described by the Marmottant model and the properties of the wall correspond to walls of OptiCell chambers commonly used in experiments. It has been found that contact with the wall can considerably change the intensities of the fundamental component and the second harmonic in the spectrum of the bubble scattered pressure relatively to their values in an unbounded liquid.

1 Introduction

Interest in the problem under study is motivated by the fact that both *in vitro* and *in vivo*, the dynamics of contrast agent microbubbles is affected by various boundaries, such as walls of experimental containers and blood vessels. Experimental data show that the proximity of boundaries can produce considerable changes in the acoustic response of a contrast microbubble [1-3]. For example, Garbin *et al*. [3] observed that the oscillation amplitude of a BR14 microbubble (Bracco Research SA, Geneva, Switzerland) was suppressed by more than 50% near the wall of an experimental OptiCell chamber (BioCrystal, Ltd., Westerville, OH). Theoretically, however, the effect of a boundary on the dynamics of a contrast microbubble is still a little-studied problem. As a matter of fact, most available theoretical models are restricted to the interaction of a bubble with a rigid wall [4-8]. In models considering other types of boundaries [9,10], it is assumed that the distance between the bubble and the wall is much larger than the radius of the bubble.

The purpose of the present study is to reveal how contact with a boundary changes the acoustic response of a contrast microbubble. To this end, a Rayleigh-Plesset-like equation is derived that describes the radial oscillation of an encapsulated bubble attached to an elastic wall. This equation is then used in numerical simulations in order to establish how contact with the wall affects the resonance properties and the scattered echo of the attached bubble.

2 Theoretical model

The geometry of the system being investigated is shown in Fig. 1. It is assumed that the bubble is surrounded by an inviscid incompressible liquid and undergoes radial and translational oscillations, remaining in contact with the wall all the time. The effect of the wall is allowed for by using the method of image sources. Namely, instead of the wall,

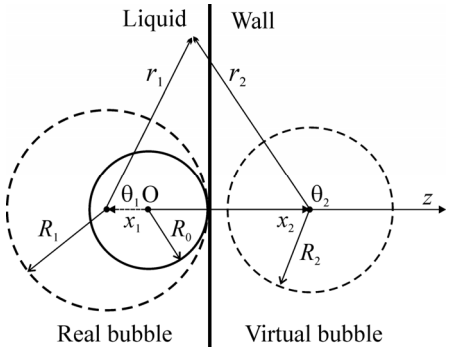

Figure 1: An encapsulated bubble oscillating in contact with an elastic wall.

a virtual bubble is introduced, assuming that the moving center of this bubble is at the same distance from the liquid-wall interface as the moving center of the real bubble and the radii of the bubbles are related by $R_2(t) = \varepsilon R_1(t)$, where ε is a constant.

2.1 Scattered field in the liquid

The velocity potential in the liquid can be represented as $\varphi_L = \varphi_1 + \varphi_2$, where φ_1 and φ_2 are given by

$$\varphi_1 = \sum_{n=0}^{\infty} a_{1n}(t)\left(R_1/r_1\right)^{n+1} P_n(\cos\theta_1) \tag{1a}$$

$$= \sum_{n=0}^{\infty} b_{1n}(t)\left(r_2/d\right)^{n} P_n(\cos\theta_2)\,, \tag{2b}$$

$$\varphi_2 = \sum_{n=0}^{\infty} a_{2n}(t)\left(R_1/r_2\right)^{n+1} P_n(\cos\theta_2) \tag{2a}$$

$$= \sum_{n=0}^{\infty} b_{2n}(t)\left(r_1/d\right)^{n} P_n(\cos\theta_1)\,. \tag{2b}$$

Here, P_n is the Legendre polynomial and $d = 2R_1$ is the distance between the bubble centers. Equations (1b) and (2b) are used to satisfy the boundary conditions on the bubble surfaces. The functions b_{1n} and b_{2n} can be expressed in terms of a_{1n} and a_{2n} by using mathematical identities that establish linkage between spherical harmonics in different coordinates [11]. The result is the following:

$$b_{jn} = (-1)^{n(2-j)} \sum_{m=0}^{\infty} \frac{(-1)^{m(j-1)} C_{nm}}{2^{m+1}}\, a_{jm}\,, \tag{3}$$

where $j = 1,2$ and $C_{nm} = (n+m)!/(n!m!)$. The functions a_{1n} and a_{2n} are found using the boundary conditions for the normal component of the liquid velocity at the surfaces of the bubbles, which are written as

$$\frac{\partial \varphi_L}{\partial r_j} = \dot{R}_j + \dot{x}_j \cos\theta_j \quad \text{at} \quad r_j = R_j(t)\,, \tag{4}$$

where the overdot denotes the time derivative and $x_j(t)$ is the position of the moving center of the jth bubble on the axis z. Note that from $x_1 = R_0 - R_1$ and $x_2 - x_1 = 2R_1$ it follows that

$$\dot{x}_j = (-1)^j \dot{R}_1\,. \tag{5}$$

Substituting Eqs. (1), (2), (3), and (5) into Eq. (4), one finds that the functions a_{1n} and a_{2n} can be calculated as follows:

$$a_{jn} = -R_1 \dot{R}_1 \varepsilon^{3(j-1)} \alpha_{jn}\,. \tag{6}$$

Here, α_{jn} is a time-independent quantity given by

$$\alpha_{jn} = \frac{1}{2^n}\sum_{m=0}^{\infty}\frac{\beta_{nm}^{(j)}}{2^m}, \tag{7}$$

where $\beta_{nm}^{(j)}$ is calculated by the following recurrence equations:

$$\beta_{n0}^{(j)} = \delta_{n0} + (-1)^{2-j}\delta_{n1} + \frac{[(-1)^n\varepsilon^{2n-2}]^{j-1}\varepsilon^{3(2-j)}n(3-n)}{8(n+1)}, \tag{8}$$

$$\beta_{nm}^{(j)} = \sum_{k=0}^{[(m-1)/2]} D_{nk}^{(j)}\beta_{k(m-2k-1)}^{(j)} \quad \text{for} \quad m>0. \tag{9}$$

Here, δ_{nm} is the Kronecker delta, [(*m*-1)/2] means the integer part of (*m*-1)/2, and

$$D_{nk}^{(j)} = \frac{[(-1)^{n+k}\varepsilon^{2n+1}]^{j-1}n}{n+1}\sum_{m=1}^{\infty}\frac{mC_{nm}C_{mk}\varepsilon^{(2m+1)(2-j)}}{(m+1)2^{2m+1}}. \tag{10}$$

2.2 Scattered field inside the wall

It is assumed that the material of the wall behaves as an elastic solid whose motion is governed by the following equation [12]:

$$\rho_W\frac{\partial^2\boldsymbol{u}}{\partial t^2} = \mu\Delta\boldsymbol{u} + (\mathrm{K}+\mu/3)\nabla(\nabla\cdot\boldsymbol{u}), \tag{11}$$

where $\boldsymbol{u}$ is the displacement vector, ρ_W is the wall density, K is the bulk modulus, and μ is shear modulus. We assume

$$\boldsymbol{u} = \nabla\varphi_W, \tag{12}$$

which means that we allow for longitudinal (compressive) waves in the wall material and neglect transverse (shear) waves. The displacement potential φ_W is taken as

$$\varphi_W = \sum_{n=0}^{\infty}c_n(t)\left(R_1/r_1\right)^{n+1}P_n(\cos\theta_1). \tag{13}$$

To find c_n, the boundary condition for the normal velocity at the liquid-wall interface is used,

$$\boldsymbol{n}\cdot\nabla\varphi_L = \boldsymbol{n}\cdot\nabla\frac{\partial\varphi_W}{\partial t}, \tag{14}$$

where $\boldsymbol{n}$ is the inward unit normal to the wall. The resulting expression for c_n is found to be

$$c_n = -\frac{R_1^2}{n+3}\left[\alpha_{1n} + (-1)^{n+1}\varepsilon^3\alpha_{2n}\right]. \tag{15}$$

2.3 Calculation of ε

To find ε, the normal force balance on the liquid-wall interface is used,

$$-p_L = \sigma_{zz} \quad \text{at} \quad r_1 = r_2, \tag{16}$$

where p_L is the time-varying pressure in the liquid and σ_{zz} is the normal component of the stress tensor of the wall material, given by [12]

$$\sigma_{zz} = \mathrm{K}(\nabla\cdot\boldsymbol{u}) + 2\mu\left(\frac{\partial u_z}{\partial z} - \frac{1}{3}\nabla\cdot\boldsymbol{u}\right). \tag{17}$$

As Eq. (16) is valid for any point on the liquid-wall interface, one can use the limiting form of this equation at $r_1 = r_2 \to \infty$. In this limit, the expressions for p_L and σ_{zz} take the following form:

$$p_L = \frac{\rho_L(1+\varepsilon^3)}{r_1}\frac{d}{dt}\left(R_1^2\dot{R}_1\right), \tag{18}$$

$$\sigma_{zz} = \frac{\beta(\varepsilon^3-1)}{r_1}\frac{d}{dt}\left(R_1^2\dot{R}_1\right), \tag{19}$$

where ρ_L is the liquid density and β is given by

$$\beta = \rho_W\frac{3\mathrm{K}-2\mu}{3\mathrm{K}+4\mu} = \frac{\rho_W\nu}{1-\nu}, \tag{20}$$

with ν denoting Poisson's ratio. Substitution of Eqs. (18) and (19) into Eq. (16) yields

$$\varepsilon = \sqrt[3]{\frac{\beta-\rho_L}{\rho_L+\beta}}. \tag{21}$$

2.4 Equation for the bubble radius

To obtain the equation for $R_1(t)$, we apply the method of the Lagrangian formalism. Recall that the presence of the elastic wall is replaced with the presence of a virtual bubble. As a result, we get the system of two bubbles surrounded by an infinite liquid identical to the liquid surrounding the real bubble. The kinetic energy of this system is given by

$$T = \frac{\rho_L}{2}\int_V(\nabla\varphi_L)^2dV, \tag{22}$$

where V is the volume occupied by the liquid. Equation (22) can be recast to

$$T = -\pi\rho_L R_1^2\dot{R}_1\int_0^{\pi}\varphi_L\big|_{r_1=R_1}(1-\cos\theta_1)\sin\theta_1 d\theta_1 - \pi\rho_L R_1^2\dot{R}_1\varepsilon^2\int_0^{\pi}\varphi_L\big|_{r_2=\varepsilon R_1}(\varepsilon+\cos\theta_2)\sin\theta_2 d\theta_2. \tag{23}$$

The calculation of Eq. (23) gives the following result:

$$T = \frac{\pi}{3}\rho_L R_1^3\dot{R}_1^2E(\varepsilon), \tag{24}$$

where the function $E(\varepsilon)$ is defined as

$$E(\varepsilon) = 6+5\varepsilon^3+6\varepsilon^5+(\varepsilon^3-2)\alpha_{11}+\varepsilon^3\alpha_{21} + \varepsilon^3\sum_{n=2}^{\infty}\frac{5-n}{2^{n+1}}\left[\alpha_{1n}+(-1)^n\alpha_{2n}\right]. \tag{25}$$

The potential energy of the system can be written as

$$U = -\frac{4\pi}{3}\left[R_1^3P_1+R_2^3P_2\right] = -\frac{4\pi R_1^3}{3}\left[P_1+\varepsilon^3P_2\right], \tag{26}$$

where P_1 and P_2 are pressures that do work on the real bubble and on the virtual bubble, respectively. The virtual bubble is assumed to experience the same pressure amplitude, i.e., $|P_2|=|P_1|$, but the pressure sign can be opposite. If the bubbles pulsate in phase, $\varepsilon > 0$ and $P_2 = P_1$.

If they pulsate out of phase, $\varepsilon < 0$ and $P_2 = -P_1$. As a consequence, Eq. (26) becomes

$$U = -\frac{4\pi}{3} R_1^3 P_1 (1+|\varepsilon|^3). \quad (27)$$

Substituting Eqs. (24) and (27) into the Lagrangian function $L = T - U$ and then into the Lagrangian equation,

$$\frac{d}{dt}\frac{\partial L}{\partial \dot{R}_1} - \frac{\partial L}{\partial R_1} = 0, \quad (28)$$

one obtains the following equation for the bubble radius:

$$R_1 \ddot{R}_1 + \frac{3}{2}\dot{R}_1^2 = \frac{P_1(t)}{\rho_L \tau(\varepsilon)}, \quad (29)$$

where the function $\tau(\varepsilon)$ is given by

$$\tau(\varepsilon) = \frac{E(\varepsilon)}{6\left(1+|\varepsilon|^3\right)}. \quad (30)$$

The pressure $P_1(t)$ can be written as

$$P_1 = P_{G0}\left(\frac{R_0}{R_1}\right)^{3\gamma} - 4\eta_L \frac{\dot{R}_1}{R_1} - P_0 - P_{ac} - S, \quad (31)$$

where P_{G0} is the equilibrium gas pressure inside the real bubble, γ is the ratio of specific heats of the gas, η_L is the shear viscosity of the liquid, P_0 is the hydrostatic pressure in the liquid, P_{ac} is the driving acoustic pressure, and the term S describes the effect of encapsulation. Note that in modern encapsulation models, such as [13] and [14], the surface tension term is incorporated into the model formulation. Therefore, we do not include it explicitly in Eq. (31).

The scattered pressure produced by the bubble in the far-field zone, i.e., at $r_1 >> R_1$, can be evaluated from Eq. (18), substituting the value of ε from Eq. (21). The resulting expression is as follows:

$$p_L(r_1 >> R_1) = \frac{\rho_L (R_1^2 \ddot{R}_1 + 2R_1 \dot{R}_1^2)}{r_1} \frac{2\beta}{\rho_L + \beta}. \quad (32)$$

3 Numerical simulations

Equation (29) shows that for a bubble being in contact with a wall, the liquid density gains a dimensionless factor τ that depends on the mechanical properties of the wall. As a consequence, the bubble oscillates as if it were in a liquid with an effective density $\rho_{\text{eff}} = \tau\rho_L$. Depending on the wall properties, τ can be either larger or smaller than 1 so the effective density can be either higher or lower than the real liquid density. This means that the resonance frequency of an attached bubble can be respectively lower or higher than the resonance frequency of the same bubble in an unbounded liquid.

In the limiting case of a rigid wall, $\beta \to \infty$, $\varepsilon = 1$, and Eq. (30) gives $\tau = 1.48984$. For real walls, values of τ are smaller. As an example, let us consider the wall of an OptiCell chamber. Such chambers are widely used in experiments on contrast agent microbubbles [3,15]. OptiCell chambers have polystyrene walls with the following mechanical parameters: $\rho_W = 1060$ kg/m^3, K = 3.75 GPa, and $\mu = 1.34$ GPa. In the case that the adjacent liquid is water with $\rho_L = 1000$ kg/m^3, one gets $\tau = 0.622024$. Differences in the behavior of a contrast agent microbubble attached to a rigid wall and that of the same bubble attached to an OptiCell wall are illustrated in Fig. 2. The simulations have been carried out by means of the program package MATHEMATICA (Wolfram Research, Inc., Champaign, IL). The following values of the physical parameters were used: $P_0 = 101.3$ kPa, $\eta_L = 0.001$ Pa·s, the surface tension of water $\sigma_L = 0.072$ N/m, the sound speed $c = 1500$ m/s, and $\gamma = 1.07$. The effect of encapsulation on the dynamics of the bubble was simulated by the shell model developed by Marmottant *et al.* [13]. A modification of this model proposed by Overvelde *et al.* [15] was used. The values of the shell parameters for the Marmottant model were also adopted from [15]: shell viscosity $\kappa_S = 0.6\times10^{-8}$ kg/s, shell elasticity $\chi = 2.5$ N/m, and initial surface tension $\sigma(R_0) = 0.02$ N/m. These values were obtained in [15] for the phospholipid-shelled contrast agent BR-14. The equilibrium gas pressure in Eq. (31) was calculated as $P_{G0} = P_0 + 2\sigma(R_0)/R_0$. The bubble resting radius was set equal to 2 μm. The bubble was insonified with a 10-cycle, 40 kPa Gaussian pulse with a center frequency in the range 1.0 – 4.5 MHz. The parameters of the pulse correspond to the conditions under which the values of the shell parameters were evaluated in [15].

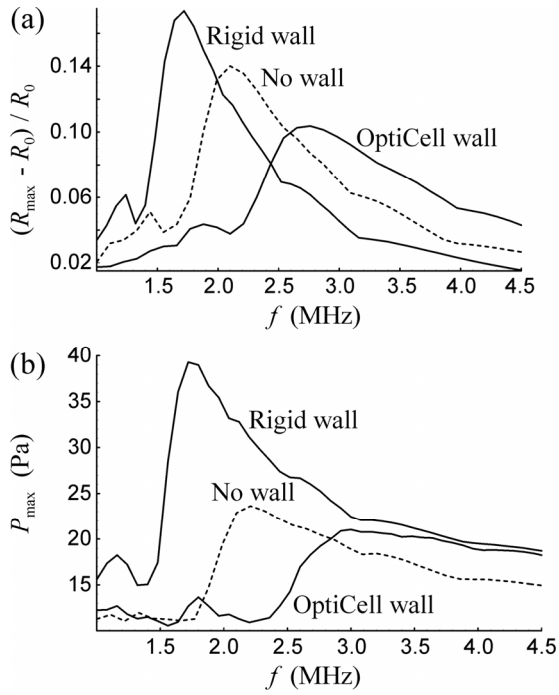

Figure 2: Resonance curves for (a) the radial oscillation and (b) the scattered pressure of an encapsulated microbubble oscillating in an unbounded liquid (dashed line), in contact with a rigid wall, and in contact with an OptiCell wall.

Figure 2(a) shows resonance curves for the bubble radial oscillation. $R_{\max}$ denotes the maximum value of the bubble radius $R(t)$ during the oscillation. The dashed line corresponds to the bubble in an unbounded liquid. Figure 2(b) shows resonance curves for the scattered pressure of the bubble in the far-field zone. $P_{\max}$ stands for the peak amplitude of the scattered pressure calculated by Eq. (32) at $r_1 = 0.01$ m. As one can see in Fig. 2, contact with the rigid wall decreases the resonance frequency of the bubble as compared to its resonance frequency in an

unbounded liquid, whereas contact with the OptiCell wall increases the resonance frequency of the bubble. The bubble oscillation amplitude can either decrease or increase depending on the value of the driving frequency. Figure 2(a) shows that the resonance frequency of a 2-μm-radius bubble with the Marmottant shell is about 2.1 MHz in an unbounded liquid. If the bubble is driven at, say, 1.9 MHz, contact with the rigid wall will increase the oscillation amplitude of the bubble, whereas contact with the OptiCell wall will decrease it. At 3 MHz, the reverse is true. These results suggest that the model of a rigid wall appears not to be an adequate approximation for walls occurring in most applications associated with contrast agent microbubbles.

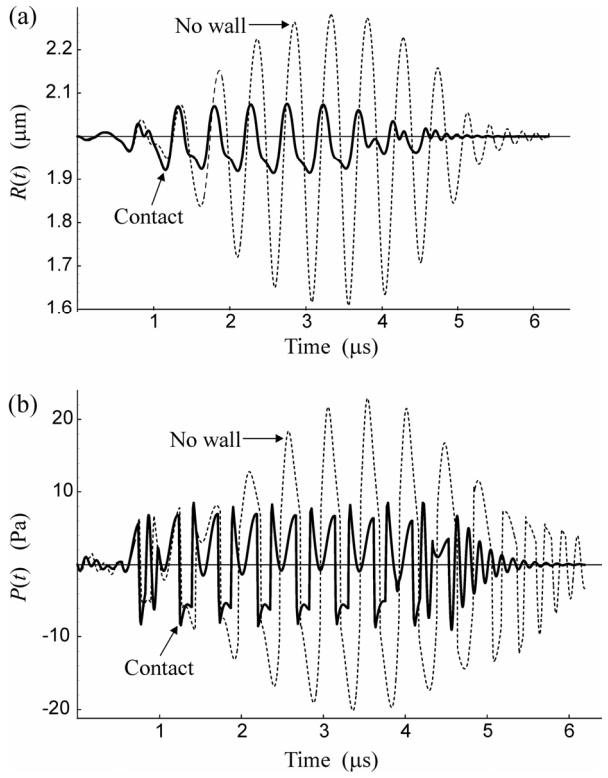

Figure 3: Examples of (a) radius-time and (b) pressure-time curves for a 2-μm-radius encapsulated bubble oscillating in an unbounded liquid and in contact with an OptiCell wall.

Figure 3 provides examples of radius-time and pressure-time curves for the same bubble as in Fig. 2. It is assumed that the bubble is insonified with a 10-cycle, 40 kPa, 2.1 MHz Gaussian pulse. It is of interest to note that the "Contact" curve in Fig. 3(a) shows the initiation of the second harmonic in the bubble oscillation. The nonlinearity of Eq. (32) increases this effect in the scattered pressure as follows from the "Contact" curve in Fig. 3(b). The Fourier spectra of the pressure-time curves shown in Fig. 3(b) are presented in Fig. 4. The spectra are normalized to the magnitude of the fundamental component of the spectrum for the bubble in contact with the wall. Figure 4 confirms that in the case being considered, contact with the OptiCell wall gives rise to a strong second harmonic which even predominates over the fundamental component. This apparently occurs because contact with the wall shifts the bubble resonance frequency so that it becomes closer to twice the driving frequency and hence more favorable conditions for the development of the second harmonic are created.

It is worth noting that Eq. (29) can be used even if the mechanical properties of a wall are unknown. In this case, the value of τ can be evaluated by fitting simulated radius-time curves to experimental data. Setting first $\tau = 1$ and fitting the experimental radius-time curve of a contrast bubble being far away from a wall in question, one can evaluate the shell parameters of this bubble. Then, fitting the experimental radius-time curve of the same bubble being in contact with the wall, one can find the value of τ characterizing the mechanical properties of the wall.

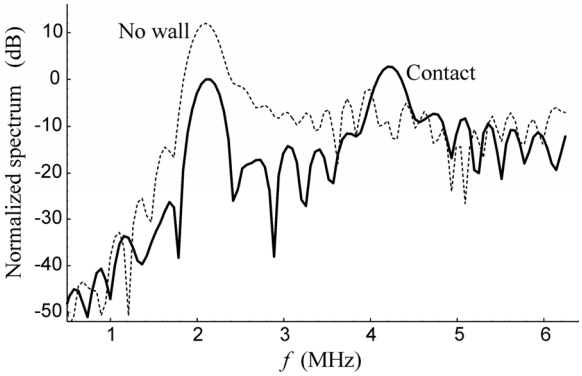

Figure 4: Fourier spectra of the pressure-time curves shown in Fig. 3(b).

4 Conclusion

A Rayleigh-Plesset-like equation has been derived that describes the radial oscillation of an encapsulated bubble attached to an elastic wall. It has been found that the liquid density in this equation gains a dimensionless factor τ that is dependent on the mechanical properties of the wall and the density of the adjacent liquid. As a result, contact with the wall affects the bubble oscillation as if the bubble oscillated in a liquid with an effective density $\rho_{\text{eff}} = \tau\rho_L$. In the limiting case of a rigid wall, $\tau = 1.48984$. For real walls, τ is smaller. In particular, for polystyrene walls of OptiCell chambers used in experiments, if the adjacent liquid is water, $\tau = 0.622024$. Thus, depending on the wall properties, τ can be either larger or smaller than 1. This means that the effective density can be either higher or lower than the real liquid density and hence the resonance frequency of an attached bubble can be respectively lower or higher than the resonance frequency of the same bubble in an unbounded liquid.

Numerical simulations have been made for a bubble with shell properties similar to those used in the Marmottant shell model. The simulations have shown that contact with the rigid wall decreases the resonance frequency of the bubble as compared to its resonance frequency in an unbounded liquid, whereas contact with the OptiCell wall increases the resonance frequency of the bubble. It has also been found that the oscillation amplitude of the bubble attached to the OptiCell wall can either decrease or increase depending on the value of the driving frequency. The simulations also revealed that contact with the wall can considerably change the intensities of the fundamental component and the second harmonic in the spectrum of the bubble scattered pressure relatively to their magnitudes in an unbounded liquid.

In closing, it should be noted that the proposed theory ignores the viscous properties of the wall and the occurrence of transverse waves. It is not improbable that these effects may be of importance and hence the development of a theory that would take them into account could be of great interest.

References

[1] M. Lankford, C. Z. Behm, J. Yeh, A. L. Klibanov, P. Robinson, J. R. Lindner, "Effect of microbubble ligation to cells on ultrasound signal enhancement: implications for targeted imaging", *Invest. Radiol*. 41(10), 721-728 (2006)

[2] S. Zhao, D. E. Kruse, K. W. Ferrara, P. A. Dayton, "Acoustic response from adherent targeted contrast agents", *J. Acoust. Soc. Am*. 120(6), EL63-EL69 (2006)

[3] V. Garbin, D. Cojoc, E. Ferrari, E. Di Fabrizio, M. L. J. Overvelde, S. M. van der Meer, N. de Jong, D. Lohse, M. Versluis, "Changes in microbubble dynamics near a boundary revealed by combined optical micromanipulation and high-speed imaging", *Appl. Phys. Lett*. 90(11), 114103 (2007)

[4] M. Strasberg, "The pulsation frequency of nonspherical gas bubbles in liquids", *J. Acoust. Soc. Am*. 25(3), 536-537 (1953)

[5] J. E. Blue, "Resonance of a bubble on an infinite rigid boundary", *J. Acoust. Soc. Am*. 41(2), 369-372 (1967)

[6] A. Shima, Y. Tomita, "The behavior of a spherical bubble near a solid wall in a compressible liquid", *Ingenieur-Archiv* 51(3-4), 243-255 (1981)

[7] E. M. B. Payne, S. J. Illesinghe, A. Ooi, R. Manasseh, "Symmetric mode resonance of bubbles attached to a rigid boundary", *J. Acoust. Soc. Am*. 118(5), 2841-2849 (2005)

[8] A. A. Doinikov, S. Zhao, P. A. Dayton, "Modeling of the acoustic response from contrast agent microbubbles near a rigid wall", *Ultrasonics* 49(2), 195-201 (2009)

[9] A. A. Doinikov, L. Aired, A. Bouakaz, "Acoustic response from a bubble pulsating near a fluid layer of finite density and thickness", *J. Acoust. Soc. Am*. 129(2), 616-621 (2011)

[10] A. A. Doinikov, L. Aired, A. Bouakaz, "Acoustic scattering from a contrast agent microbubble near an elastic wall of finite thickness", *Phys. Med. Biol*. 56(21), 6951-6967 (2011)

[11] A. A. Doinikov, "Translational motion of two interacting bubbles in a strong acoustic field", *Phys. Rev. E* 64(2), 026301 (2001)

[12] L. D. Landau, E. M. Lifshitz, *Theory of Elasticity*, Pergamon Press, Oxford (1970)

[13] P. Marmottant, S. van der Meer, M. Emmer, M. Versluis, N. de Jong, S. Hilgenfeldt, D. Lohse, "A model for large amplitude oscillations of coated bubbles accounting for buckling and rupture", *J. Acoust. Soc. Am*. 118(6), 3499-3505 (2005)

[14] S. Paul, A. Katiyar, K. Sarkar, D. Chatterjee, W. T. Shi, F. Forsberg, "Material characterization of the encapsulation of an ultrasound contrast microbubble and its subharmonic response: Strain-softening interfacial model", *J. Acoust. Soc. Am.* 127(6), 3846-3857 (2010)

[15] M. Overvelde, V. Garbin, J. Sijl, B. Dollet, N. de Jong, D. Lohse, M. Versluis, "Nonlinear shell behavior of phospholipid-coated microbubbles", *Ultrasound Med. Biol*. 36(12), 2080-2092 (2010)